ADVANCED HEALTHCARE MATERIALS
www.advhealthmat.de

Glioblastoma Cell Lysate and Adjuvant Nanovaccines via Strategic Vaccination Completely Regress Established Murine Tumors

Songsong Zhao, Yanyi Qu, Zhiwei Sun, Shuo Zhang, Mingyu Xia, Yan Shi, Jingyi Wang, Yuan Wang, Zhiyuan Zhong, and Fenghua Meng**

Tumor vaccines have shown great promise for treating various malignancies; however, glioblastoma (GBM), characterized by its immunosuppressive tumor microenvironment, high heterogeneity, and limited accessibility, has achieved only modest clinical benefits. Here, it is reported that GBM cell lysate nanovaccines boosted with TLR9 agonist CpG ODN (GlioVac) via a strategic vaccination regimen achieve complete regression of malignant murine GBM tumors. Subcutaneous administration of GlioVac promotes uptake by cervical lymph nodes and antigen presentation cells, bolstering antigen cross-presentation and infiltration of GBM-specific $CD8^+$ T cells into the tumor. Notably, a regimen involving two subcutaneous and three intravenous vaccinations not only activates systemic anti-GBM immunity but also further enhances the tumor infiltration of cytotoxic T lymphocytes, effectively reshaping the "cold" GBM tumor into a "hot" tumor. This approach led to a state of tumor-free survival in 5 out of 7 mice bearing the established GL261 GBM model with complete protection from tumor rechallenge. In an orthotopic hRas-GBM model induced by a lentiviral plasmid, GlioVac resulted in ≈100% complete tumor regression. These findings suggest that GlioVac provides a personalized therapeutic vaccine strategy for glioblastoma.

1. Introduction

Glioblastoma (GBM) with a highly invasive nature is one of the most lethal primary malignancies.[1] Standard treatment for GBM patients generally involves surgical resection, high-dose radiotherapy, and temozolomide chemotherapy, yet these approaches are often limited by rapid recurrence, with a median overall survival of less than 15 months.[2] In recent years, therapeutic vaccines based on dendritic cells (DCs), peptide antigens, neoantigens, and mRNA that stimulate adaptive anti-cancer immunity have appeared as a new treatment modality for GBM patients.[3] Currently, there are over 40 ongoing clinical trials evaluating the efficacy of anti-GBM vaccine therapies.[4] For example, the DC vaccine DCVax-L nearly doubled the 48 month survival rate of GBM patients in a pivotal phase III clinical trial.[5] Similarly, the peptide vaccine SurVaxM has shown promise in a phase II clinical trial, prolonging median overall survival from 14.8 to 30.6 months.[6] In spite of clear clinical benefits, existing tumor vaccines are unable to prevent GBM recurrence, which can be attributed to the innate tumor heterogeneity, an immunosuppressive tumor microenvironment (TME), low T cell infiltration, and inadequate immune activation, all of which contribute to GBM's immune evasion.[7]

Nanovaccines that co-deliver tumor antigens and immunoadjuvants to immune organs and antigen-presenting cells (APCs) have shown great potential in boosting anti-cancer immunity across various tumor models.[8] Whole tumor cell nanovaccines, in particular, have been reported to be able to effectively address the challenge of incomplete tumor antigen coverage.[9] However, there are very few reports on the delivery of GBM nanovaccines to cervical lymph nodes (CLNs),[10] which is the key organ for brain immune surveillance. Evidence suggests that GBM is associated with both local immunosuppression and systemic T-cell sequestration in the bone marrow.[11] This interplay of local and systemic immune dysregulation significantly compromises the recruitment of tumor-infiltrating T cells, facilitating immune evasion in GBM.

Here, we report that glioblastoma cell lysate nanovaccines boosted with Toll-like receptor-9 agonist CpG ODN (GlioVac) via a strategic vaccination regimen completely regress malignant murine GBM tumors (Scheme 1). The nanovaccines are comprised of chimaeric polymersomes that efficiently load tumor cell

S. Zhao, Y. Qu, Z. Sun, M. Xia, Y. Shi, J. Wang, Z. Zhong, F. Meng
Biomedical Polymers Laboratory
College of Chemistry
Chemical Engineering and Materials Science
and State Key Laboratory of Radiation Medicine and Protection
Soochow University
Suzhou 215123, P. R. China
E-mail: zyzhong@suda.edu.cn; fhmeng@suda.edu.cn
S. Zhang, Y. Wang, Z. Zhong
College of Pharmaceutical Sciences
Soochow University
Suzhou 215123, P. R. China

The ORCID identification number(s) for the author(s) of this article can be found under https://doi.org/10.1002/adhm.202500911

DOI: 10.1002/adhm.202500911

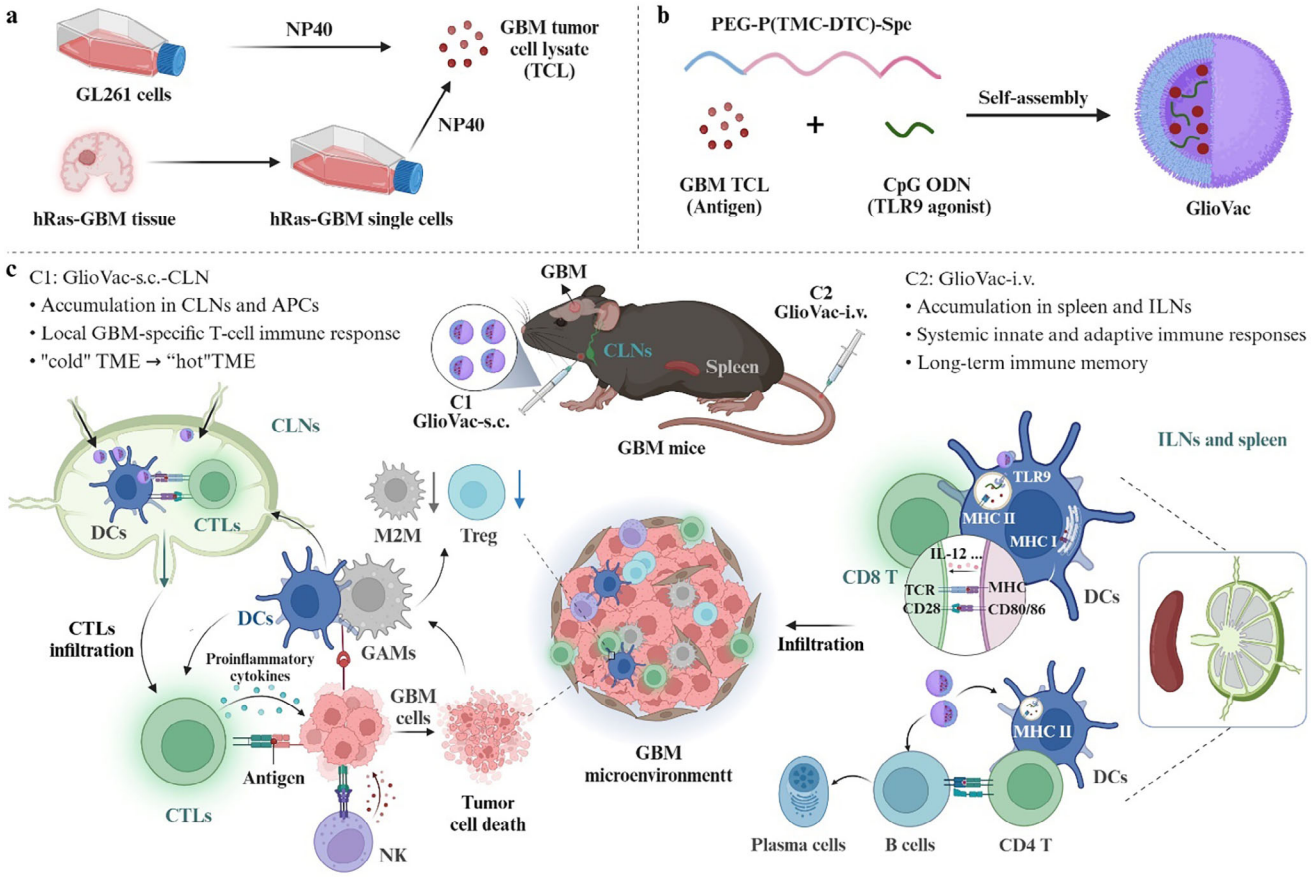

Scheme 1. Illustration of the preparation and application of GlioVac. a) Schematic of GBM antigen extraction from tumor cells lysate and b) co-loading with CpG ODN into polymersomes to yield GlioVac. c) Mechanisms of GlioVac via subcutaneous and intravenous injection sequential strategy, inducing systemic innate and adaptive immune responses against GBM.

lysates and CpG.[12] To activate both local and systemic anti-GBM immunity, the mice are vaccinated with GlioVac through two subcutaneous and three intravenous doses. Interestingly, our results demonstrate that GlioVac enhances the tumor infiltration of cytotoxic T lymphocytes, reshaping the GBM TME from "cold" into "hot", leading to 5 out of 7 mice with established GL261 GBM tumors achieving tumor-free status and full protection from tumor rechallenge. The rational vaccination regimen of GlioVac effectively induces durable local and systemic anti-GBM immunity compared to traditional subcutaneous vaccination employed clinically, providing a potent personalized tumor vaccine strategy for GBM.

2. Results and Discussion

2.1. Preparation of GlioVac

GlioVac was formulated by co-loading GBM tumor cell lysate (TCL) and the TLR9 agonist CpG into chimaeric polymersomes composed of poly(ethylene glycol)-b-poly(trimethylene carbonate-co-dithiolane trimethylene carbonate)-b-spermine. The murine GBM cell lysates were acquired via lysis using NP-40 lysis buffer. The co-loading process of cell lysates and CpG achieved near-quantitative encapsulation at a mass ratio of 1/1 and drug-loading contents of 5.0 wt.%. The resulting GlioVac exhibited a hydrodynamic diameter of 55 nm (PDI: 0.09) and a neutral surface charge (Table S1 and Figure S1a, Supporting Information). TEM image of GlioVac exhibited a spherical structure with an average size of ≈55 nm (Figure S1b, Supporting Information). Empty polymersomes (vehicle), TCL-loaded polymersomes (NanoAg), and CpG-loaded polymersomes (NanoCpG) all exhibited similar sizes. GlioVac showed excellent stability under various conditions, including storage, dilution, and 10% serum solution (Figure S1c, Supporting Information). In the presence of 10 mM glutathione (GSH), GlioVac revealed a rapid increase in size (Figure S1d, Supporting Information), a reduction-responsiveness that was further validated by agarose gel electrophoresis (Figure S1e, Supporting Information). The stability and GSH-sensitivity of GlioVac are attributable to the encapsulation of tumor cell lysates and CpG within the polymersome interior, as well as the disulfide-crosslinking of the membrane, consistent with previous reports.[12b]

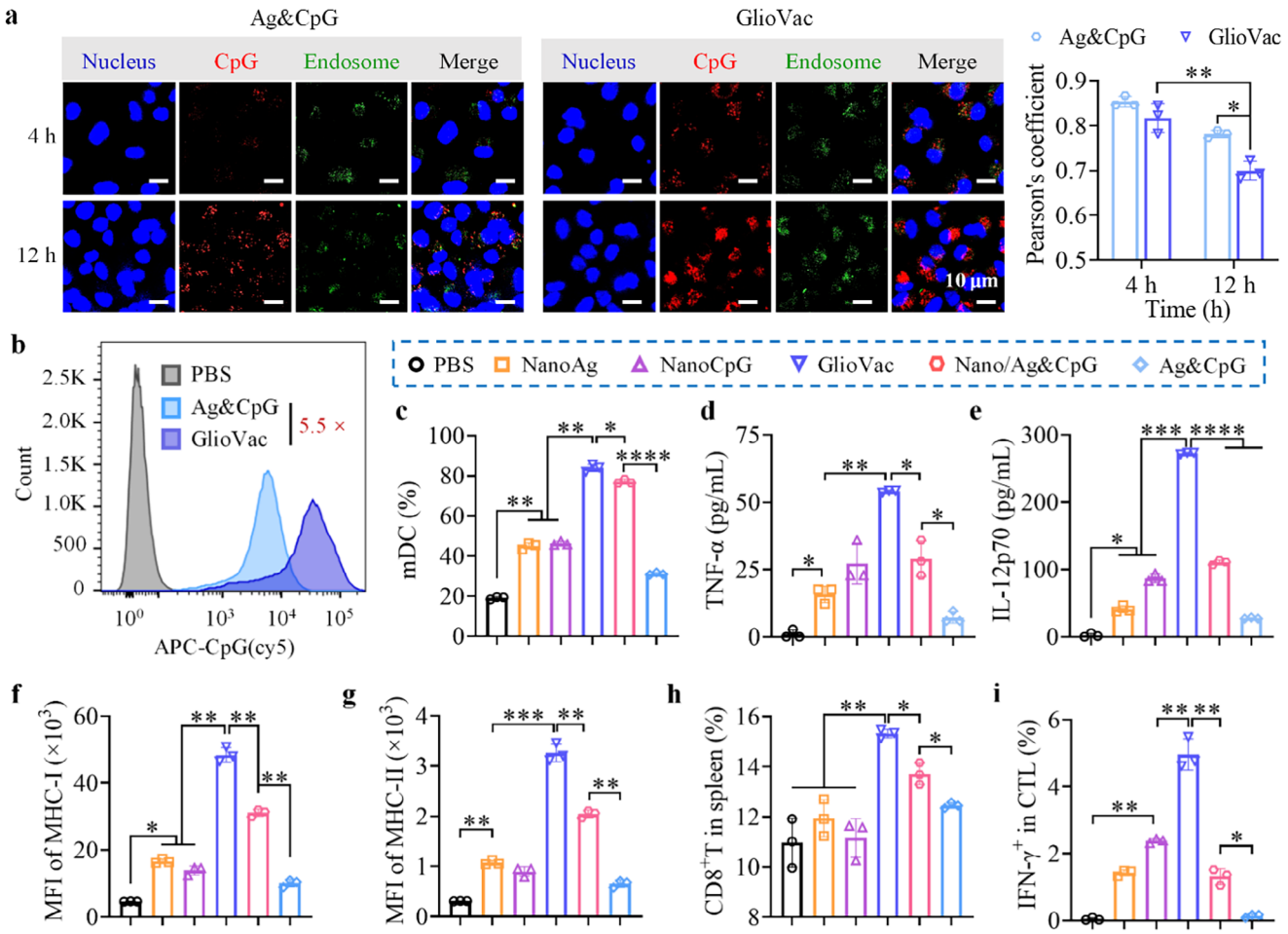

Figure 1. In vitro cellular uptake and stimulation of BMDCs by GlioVac. a) CLSM studies of uptake and colocalization of GlioVac with endosomes of BMDCs at 4 and 12 h incubation ($n = 3$), and b) flow cytometry analysis of cellular uptake of GlioVac by BMDCs at 4 h incubation, using free Ag&CpG as control and cy5-CpG as a probe. c) Percentages of mDCs ($CD11c^+CD80^+CD86^+$) in total BMDCs ($CD11c^+$), secretion of d) TNF-α and e) IL-12p70 in the medium, and mean fluorescence intensity (MFI) of f) MHC-I and g) MHC-II in total BMDCs at 24 h incubation with GlioVac ($n = 3$). Percentages of h) $CD8^+$T (CTLs) in the spleen and i) IFN-γ^+CTL in CTLs at 48 h incubation with GlioVac ($n = 3$). For c-i, antigen and CpG in GlioVac: 1 μg mL^{-1}. $^*p < 0.05$, $^{**}p < 0.01$, $^{***}p < 0.001$, $^{****}p < 0.0001$.

2.2. Activation and Antigen Presentation of DCs and T cell Response In Vitro

To study the stimulation of APCs, antigen presentation, and subsequent T-cell activation in vitro, bone marrow-derived dendritic cells (BMDCs) were treated with GlioVac. Cy5-labeled CpG (cy5-CpG) was used as a probe to assess cellular uptake in BMDCs. CLSM and flow cytometry analysis demonstrated that GlioVac showed a 5.5-fold increase in endocytosis in BMDCs compared to the physical mixture of free Ag and CpG (denoted as Ag&CpG) (**Figure** 1a,b). GlioVac also demonstrated efficient endosomal escape showing a decreased colocalization with endo/lysosome markers, reflected in the Pearson's coefficient from 4 h to 12 h (**). This phenomenon is attributed to the prone-sponge effect and the binding of CpG with TLR9 within the endo/lysosomal membrane.[13] Such mechanisms likely contribute to the heightened immune activation and antigen presentation.

As expected, GlioVac induced 85% BMDCs into mature DCs (mDC, $CD80^+CD86^+$), significantly surpassing the levels in control groups (Figure 1c). This maturation was accompanied by significant cytokine secretion, with tumor necrosis factor-alpha (TNF-α) and interferon-12p70 (IL-12p70) levels increased by 2.0–2.7 fold and 2.1–9.6 fold, respectively (Figure 1d,e). Interestingly, both major histocompatibility complex (MHC) I and MHC II expressions on BMDCs were upregulated by factors of 2.5–5 compared to monotherapies and free counterparts (Figure 1f,g), indicating a great capacity for presenting various antigens to T cells and facilitating cross-presentation of tumor antigens.[14]

To further investigate Tcell activation, splenic T cells were co-cultured with DCs presenting tumor antigens. Flow cytometry results demonstrated that GlioVac significantly promoted the proliferation of cytotoxic T lymphocytes (CTLs, $CD8^+$T) compared to monotherapies and other control groups (Figure 1h), confirming its exceptional antigen cross-presentation capability.[14b,15] The content of IFN-γ^+CTLs was notably augmented by 2.5 to 50 fold relative to controls (Figure 1i). Notably, GlioVac exhibited superior efficacy in DC activation, antigen presentation, and T-cell stimulation compared to the mixture of vehicle and free Ag&CpG

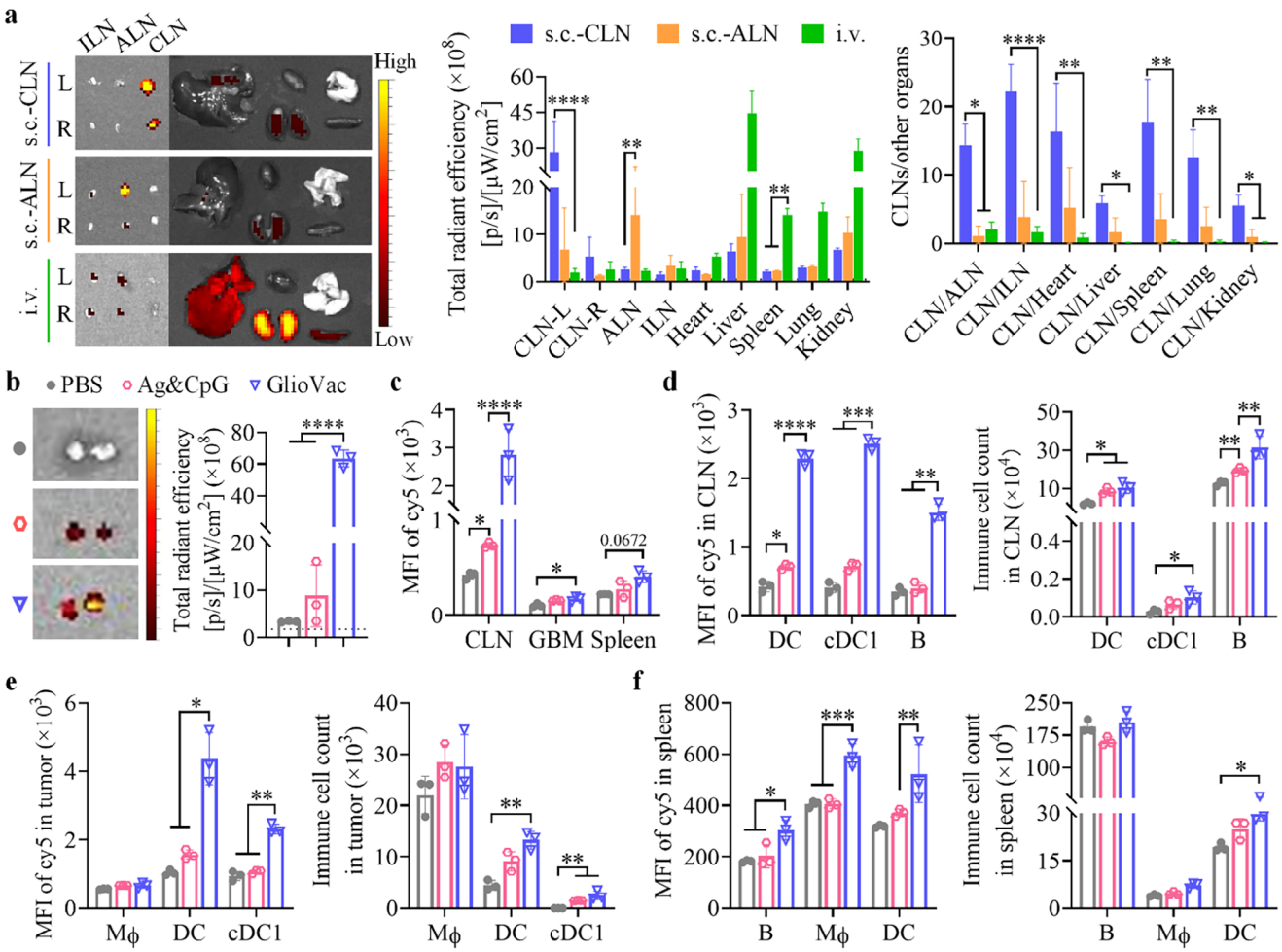

Figure 2. In vivo biodistribution studies of GlioVac in orthotopic GL261 mice upon a single injection using 1.5 wt.% cy5-CpG as a probe ($n = 3$). a) Ex vivo imaging and semi-quantification of GlioVac in CLNs, ALNs, ILNs and major organs, and the ratios of accumulation in CLNs/other organs at 12 h post a single injection via s.c.-CLN,s.c.-ALN, or i.v. route. b) Ex vivo imaging and semi-quantification of GlioVac in CLNs at 12 h post-injection via s.c.-CLN. c) MFI of cy5 uptaken by single cells of CLN, tumor, and spleen tissues. d) MFI of cy5 uptake by DCs, cDC1, and B cells in CLNs and the corresponding cell counts. e) MFI of Cy5 uptake by Mϕ, DCs, and cDC1 in tumor and the corresponding cell counts. f) MFI of Cy5 uptake by B cells, Mϕ, and DCs in spleen and the corresponding cell counts. $^{*}p < 0.05$, $^{**}p < 0.01$, $^{***}p < 0.001$, and $^{****}p < 0.0001$.

(Nano/Ag&CpG), confirming the crucial role of co-delivery of both Ag and CpG in promoting highly efficient antigen presentation and subsequent immune stimulation.

2.3. Accumulation of GlioVac in CLNs and APCs in Orthotopic GL261 Mice

CLNs serve as critical lymphoid organs for immune surveillance of the brain environment.[16] Efficient delivery of tumor vaccines to CLNs and APCs is considered a prerequisite for the rapid initiation of immune responses that inhibit tumor proliferation at an early stage.[17] We administered GlioVac via subcutaneous injection as close as possible to the CLNs (denoted as s.c.-CLN) in orthotopic murine GL261 tumor-bearing models (referred to as GL261 mice), which were built in C57BL/6J mice by intracranial inoculation with GL261 cells. The biodistribution of GlioVac in CLNs and major organs was investigated, comparing the CLN enrichment efficacy of subcutaneous injection near axillary lymph nodes (ALNs, denoted as s.c.-ALN) and intravenous injection (i.v.). In vivo near-infrared (NIR) imaging showed that for both s.c.-CLN and s.c.-ALN groups within 12 h, fluorescent signals were mainly concentrated near the injection sites, where the i.v. group exhibited significantly lower signals (Figure S2, Supporting Information). High levels of GlioVac enrichment were detected in the CLNs or ALNs on the injected side (left) in respective s.c.-CLN and s.c.-ALNs groups. In comparison, much lower signals were detected in contralateral CLNs or ALNs, inguinal lymph nodes (ILNs), and major organs (**Figure 2a**). Notably, the s.c.-CLN injection led to a 4.1 fold increase in CLN enrichment compared to the s.c.-ALN group. In sharp contrast, i.v. injection resulted in a high accumulation in the spleen, liver, lung, and kidney, with minimal deposition in lymph nodes. The spleen, as a crucial secondary lymphoid organ, plays a vital role in activating systemic immunity. Interestingly, the GlioVac accumulation ratios in CLN/organs demonstrated superior

selectivity for CLNs via s.c.-CLN injection, as opposed to s.c.-ALN or i.v. injection. Given the pivotal role of CLNs in enhancing GBM immunotherapy compared to ALNs,[18] our results emphasize the importance of vaccination of GlioVac via s.c.-CLN injection to facilitate robust immune surveillance against brain tumors. Additionally, the high GlioVac distribution in the spleen via i.v. injection compensates for the limitations associated with s.c.-CLN injection by greatly activating systemic immune responses against GBM and promoting the infiltration of peripheral immune cells into TME. Therefore, these two vaccination approaches may collectively enhance therapeutic efficacy and the establishment of immune memory in orthotopic GBM models.

Subsequently, we investigated the biodistribution of GlioVac in CLNs and its cellular uptake by APCs following s.c.-CLN injection using free Ag&CpG as a control. Ex vivo imaging confirmed an extraordinary enrichment of GlioVac at CLNs, showing a 7.8 fold increase compared to free Ag&CpG (Figure 2b). Flow cytometry analysis of single-cell suspensions further validated the high deposition of GlioVac within the CLNs (Figure 2c). The endocytosis of GlioVac by APCs, including DCs, B cells, and macrophages (Mϕ) in immune organs is indispensable for inducing effective antitumor immunity. Among these, DCs, the most potent professional APCs, particularly type 1 conventional dendritic cells (cDC1), are critical for antigen cross-presentation and mediating CD8 T-cell immune responses.[19] The GlioVac group showed 3.4–4.3 fold increase in mean fluorescence intensity (MFI) values for DCs, cDC1, and B cells compared to the free Ag&CpG group, in addition to increased APC proliferation in the CLNs (Figure 2d).

Interestingly, despite its low accumulation at the GBM tumor, GlioVac showed a significant increase in the uptake by DCs and cDC1- and in total cell counts (Figure 2e). This phenomenon may be attributed to the migration of peripheral DCs that internalized GlioVac into the TME. While the uptake of GlioVac by APCs in the spleen was considerably lower than in the CLNs and TME, the comprehensive total cell counts remain substantial, potentially contributing to the systemic anti-GBM immune response (Figure 2f). These results demonstrate that s.c.-CLN injection of GlioVac results in efficient accumulation in the CLNs and is predominantly internalized by DCs and B cells in CLNs, inducing a robust local immune response. GlioVac injection via s.c.-CLN was referred to GlioVac, if not stated otherwise in the following studies.

2.4. Anti-Tumor Efficacy of GlioVac in GL261 Mice

Encouraged by the significant accumulation of GlioVac in the CLN and its uptake by APCs, we sought to investigate the anti-GBM immunotherapeutic efficacy in orthotopic GL261 models. On day 3 post-inoculation, GL261 mice were vaccinated five times with GlioVac-s.c. at Ag and CpG doses of 1 and 1 mg kg^{-1}, taking Nano/Ag&CpG, NanoAg, NanoCpG, and PBS as controls (**Figure 3a**). The relative body weight and survival curve showed that GlioVac significantly inhibited GBM progression and prolonged the median survival time (MST) from 18 d (PBS group) to 36 d (***), realizing 28.6% complete tumor elimination (Figure 3b,c). The control groups receiving NanoAg, NanoCpG, and Nano/Ag&CpG only showed limited efficacy, with MSTs of 25–27 days. The results suggest the crucial importance of CLN-homing character and co-delivery of antigens and immunoadjuvants to the same APCs endowed by GlioVac in vivo, which ensure synergistic activation of strong antigen cross-presentation and GBM-specific immune responses in orthotopic models.

Recent research has indicated that the activation of systemic immunity is imperative for effective immunotherapy of GBM, particularly to counter systemic immunosuppression.[7b,20] Given the enhanced accumulation of GlioVac-i.v. in the spleen following i.v. injection, we adopted a sequential vaccination strategy involving two s.c.-CLN injections followed by three i.v. injections (referred as to GlioVac-s.c.+i.v.). GlioVac via this sequential vaccination regimen notably further prolonged the survival of GL261 mice, achieving a remarkable 71% elimination of GBM (Figure 3c). Histological analysis using hematoxylin and eosin (H&E) staining of tumor-bearing brain slices confirmed these findings, revealing a significantly reduced GBM density and increased infiltration of immune cells (Figure 3d). Furthermore, increased serum levels of proinflammatory cytokines, including IFN-γ and IL-12p70, were detected in the GlioVac-s.c.+i.v. group, with increases ranging from 1.9 to 25.2 fold compared to control groups (Figure 3e,f). While there was no upregulation of anti-inflammatory cytokine IL-10 levels (Figure 3g). In addition, GlioVac-treated mice exhibited no obvious damage in major organs (Figure S3, Supporting Information), demonstrating a good safety profile. These results confirm the superior efficacy of the rational sequential strategy of s.c.-CLN and i.v. vaccination to traditional s.c. vaccination, as well as its crucial role in orchestrating robust local and systemic anti-GBM immune responses and in inhibiting GBM progression.

2.5. Immunological Analysis of GL261 Mice Treated with GlioVac

To elucidate the mechanisms underlying the local and systemic immune responses induced by GlioVac, we conducted a comprehensive immunological analysis in GL261 mice. Immune cells from the CLNs, TME, spleen, and peripheral blood (PB) were harvested and analyzed two days after the last injection (**Figure 4a**) using gating strategies shown in Figure S4 (Supporting Information). GlioVac significantly stimulated the DC maturation and antigen presentation within CLNs and TME, showing increases of 1.3 to 2.5 fold compared to control groups (Figure 4b–e). Notably, GlioVac-s.c.+i.v. treatment showed greatly increased infiltration of cDC1 and MHC I antigen cross-presentation in the TME, with increases of 2.3 and 1.2 fold, respectively, compared to GlioVac group (Figure 4f,g). DCs, especially intratumoral cDC1s, are instrumental in acquiring tumor antigens, migrating to CLNs to activate GBM-specific $CD8^+$ T cells, and promoting the proliferation and functional efficacy of CTLs.[21] The effective DC maturation and antigen cross-presentation induced by the GlioVac-s.c.+i.v. regimen contributed to an ≈1.5–4.1 fold increase in $CD4^+$ T and $CD8^+$ T cell populations, as well as a 1.5 to 9.7 fold higher contents of effector T cells, e.g., $CD107a^+$CTLs and IFN-γ^+CTLs, compared to control groups (Figure 4h–k).

Systemic intravenous vaccination is well-documented to activate innate immunity, enhance CTL generation, and reprogram the immunosuppressive TME, leading to effective tumor repression.[11b] Immunoassays confirmed the activation of

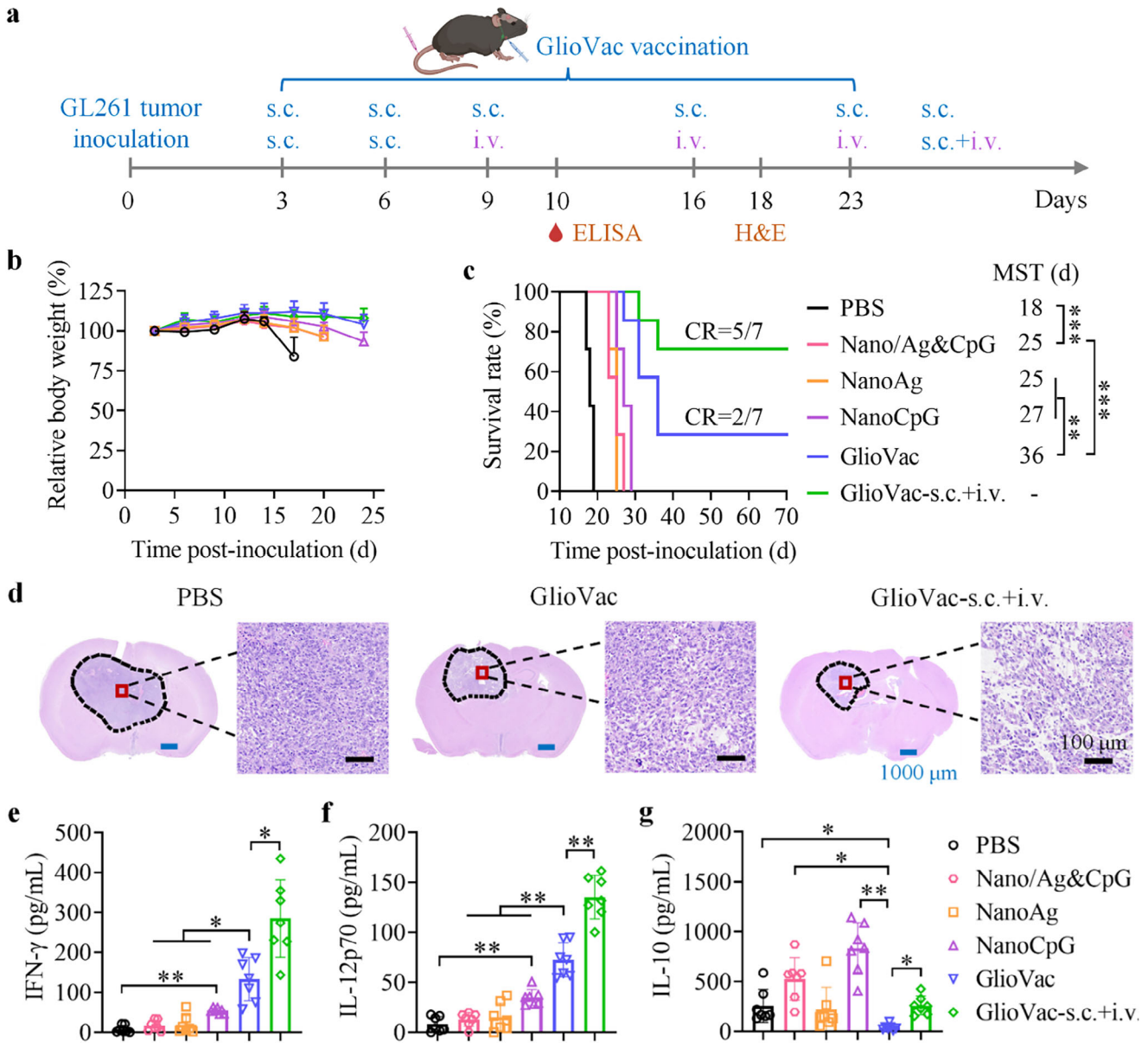

Figure 3. Therapeutic efficacy of GlioVac in orthotopic GL261 mice. a) Experimental schedule. On days 3, 6, 9, 16, and 23, mice were subcutaneously injected with GlioVac, NanoAg, NanoCpG, Nano/A&C (mixture of Vehicle and free Ag&CpG) (Ag and CpG: 1 mg kg^{-1}) or PBS. GlioVac was also administered with two s.c. injections and three i.v. injections. b) Relative body weight and c) survival curves of the mice ($n = 7$). d) H&E staining of cancerous brain slices on day 18 ($n = 1$). Blue scale bars: 1000 μm and black scale bars: 100 μm. Serum concentrations of e) IFN-γ, f) IL-12p70, and g) IL-10 on day 10 ($n = 7$). *$p < 0.05$, ** $p < 0.01$, and *** $p < 0.001$.

innate immune responses following GlioVac-s.c.+i.v. regimen, as evidenced by increased populations of natural killer (NK) cells, γδT cells, and natural killer T (NKT) cells, with fold increases of 1.7, 2.1, and 1.4, respectively (Figure 4l–n). Additionally, both GlioVac and GlioVac-s.c.+i.v. regimens significantly reduced the immunosuppressive cell populations, including regulatory T cells (Tregs) and M2 phenotype macrophages (M2M), by a factor of 1.9 compared to the PBS group (Figure 4o,p). The significant increase in the ratios of CTLs to Tregs (CTL/Treg) and M1 macrophages to M2 macrophages (M1M/M2M) within the TME (Figure 4q,r) underscores the capacity of GlioVac to reprogram immunosuppressive TME commonly associated with GBM.

The robust local immune responses elicited by GlioVac-s.c.+i.v. may be attributed to the activation of systemic immunity. The spleen and PB serve as primary sites for T-cell activation following i.v. injection. Compared to GlioVac alone, GlioVac-s.c.+i.v. regimen showed enhanced innate and adaptive immune responses, characterized by increased NK cells, $CD69^+$CTLs, $CD44^+$CTLs, and plasma cells in both spleen (**Figure** 5a–d) and PB samples (Figure 5f–i). Notably, This treatment also resulted in a notable downregulation of the depletion marker programmed

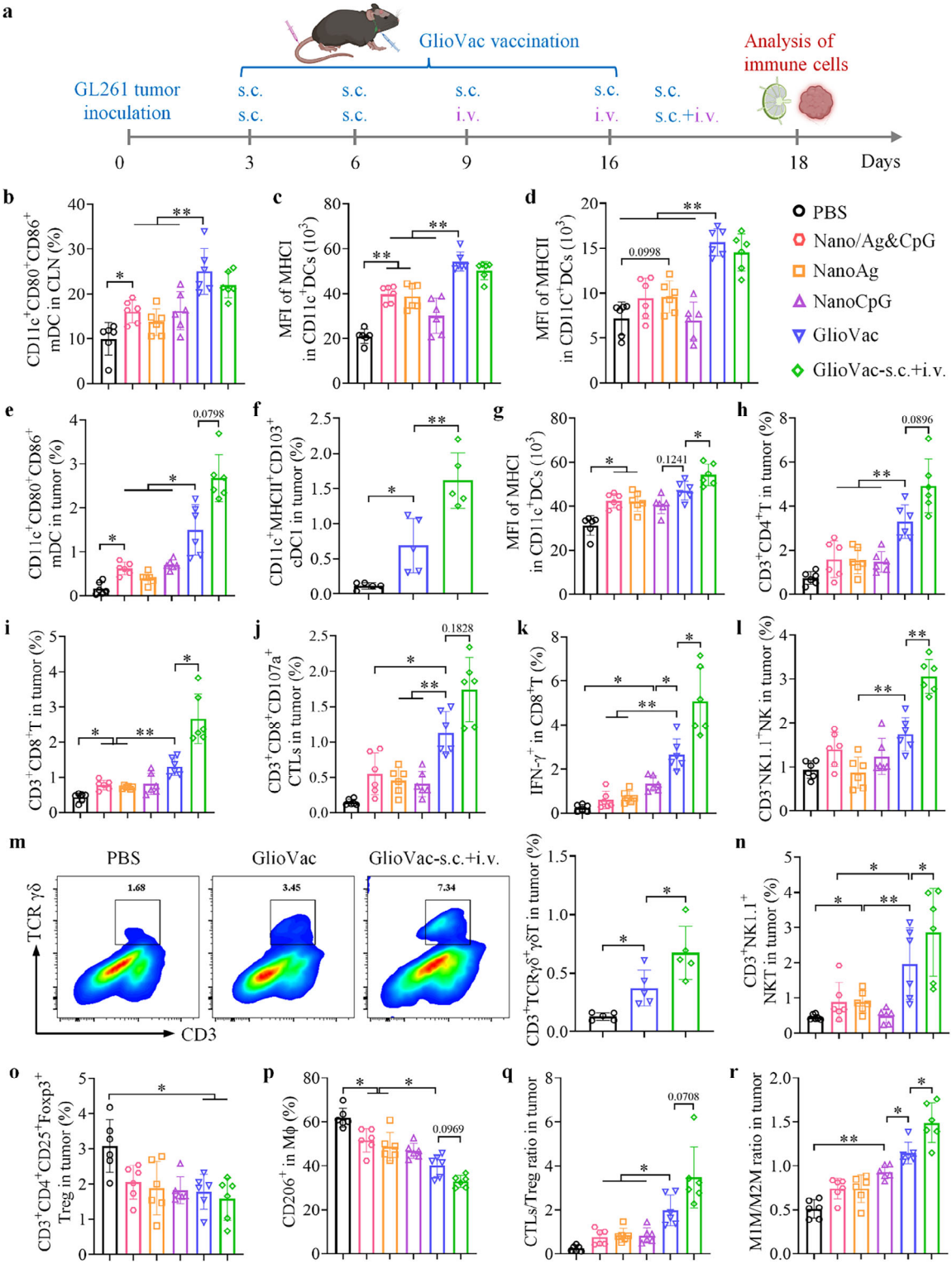

Figure 4. Analysis of local anti-tumor immune responses in orthotopic GL261 mice treated with GlioVac and GlioVac-s.c.+i.v. strategies on day 18 ($n = 6$). a) Experimental schedule. On days 3, 6, 9, and 16, mice were subcutaneously injected with GlioVac, NanoAg, NanoCpG, Nano/A&C (Ag and CpG: 1 mg kg^{-1}) or PBS. GlioVac was also administered with two s.c. injections and two i.v. injections. b) Percentages of mDCs in CLNs and their expression of c) MHC I and d) MHC II molecules in total DCs. Percentages of e) mDCs and f) cDC1s in tumor and g) MHC I expression in total DCs. Percentages of h) $CD4^+$T and i) $CD8^+$T cells (CTLs), as well as j) $CD107a^+$CTLs, k) IFN-γ^+CTLs, and l) NK cells in tumor. m) Representative flow charts and percentages of $\gamma\delta$T and of n) NKT cells in the tumor. Percentages of o) Tregs and p) M2 phenotype macrophage (M2M), as well as the ratios of q) CTLs/Treg and r) M1M/M2M in the tumor. $^*p < 0.05$, $^{**}p < 0.01$.

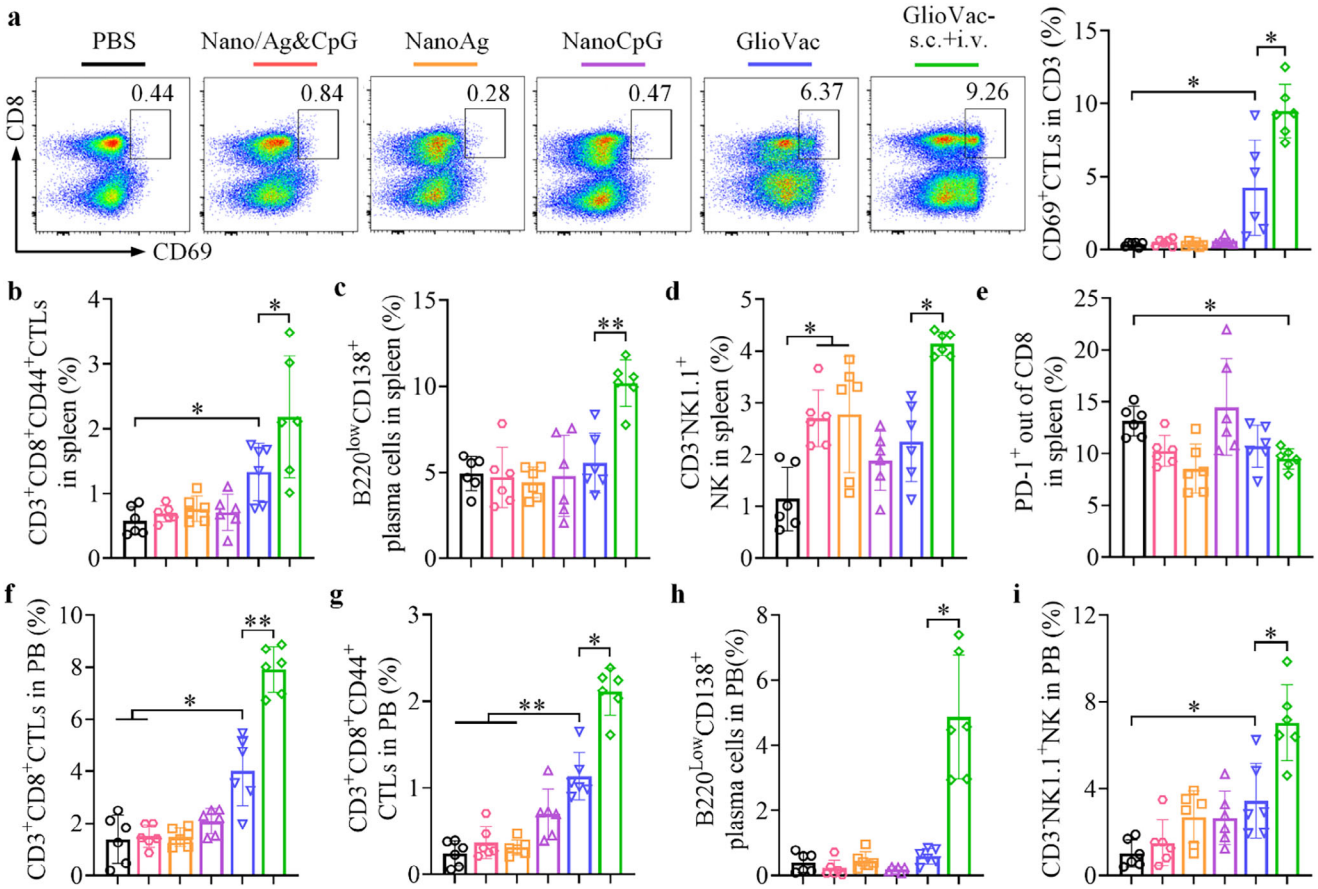

Figure 5. Analysis of systemic anti-tumor immune responses in orthotopic GL261 mice treated with GlioVac and GlioVac-s.c.+i.v. strategies as indicated in Figure 4a on day 18 ($n = 6$). a) Flow charts and percentages of $CD69^+$CTLs in the spleen. Percentages of b) $CD44^+$CTLs, c) plasma cells, d) NK cells, and e) PD-1^+CTLs in the spleen. Percentages of f) CTLs, g) $CD44^+$CTLs, h) plasma cells, and i) NK cells in the PB. $^*p < 0.05$ and $^{**}p < 0.01$.

death receptor-1 (PD-1) in splenic CTLs (*, Figure 5e), thereby mitigating the challenges associated with immune checkpoint upregulation commonly observed with many tumor vaccines.[22]

Furthermore, immunohistochemical (IHC) staining of tumor slices validated that GlioVac treatment induced high levels of APC activation (mDCs, $CD80^+$), and infiltration of CTLs ($CD3^+CD8^+$), NK cells (NKR-$P1C^+$), and M1M ($Iba1^+iNOS^+$), compared to PBS group. As anticipated, the GlioVac-s.c.+i.v. regimen further substantially amplified the infiltration of proinflammatory immune cells (Figure S5, Supporting Information). These results demonstrate that GlioVac-s.c.+i.v. effectively activates systemic innate and adaptive immunity, leading to enhanced immune cell infiltration in the tumor and reprogrammed TME to achieve the elimination of orthotopic GBM.

2.6. Long-Term Anti-GBM Immune Memory Triggered by GlioVac in GL261 Mice

We next investigated the long-term immune memory generated by GlioVac by conducting rechallenge experiments in cured GL261 mice, which received an intracranial injection of GL261-Luc cells at 80 days post-initial inoculation (**Figure 6a**). In vivo brain bioluminescence imaging showed that both GlioVac and GlioVac-s.c.+i.v. treatments significantly inhibited GBM recurrence within 17 days following rechallenge (Figure 6b). Remarkably, no intracranial tumors were observed in both groups by day 20, precluding the possibility of detailed immune cell analysis in the TME. PB and spleen samples of these mice were then collected for immunoassays, and the results demonstrated a pronounced activation of immune memory in the GlioVac-s.c.+i.v. group, characterized by an increase in central memory T cells (T_{CM}) and effector memory T cells (T_{EM}) with ca. 1.3 fold increase compared to GlioVac group (Figure 6c,d). This finding indicates the intravenous component of GlioVac-s.c.+i.v. treatment significantly enhances immune memory formation.

Moreover, splenic cells of the GlioVac-s.c.+i.v. group exhibited a remarkable capacity to induce apoptosis in GL261 cells, with a 72.2% cell death, which was 1.11 and 1.93 fold compared to the GlioVac and PBS group (Figure 6e). Interestingly, GlioVac pretreated splenic T cells of GL261 mice exhibited no cytotoxicity toward several murine cells such as BV2, bEnd.3, NIH/3T3 and MLE12 cells (cell viability >90%), affirming the excellent GBM-targeted capability and good safety profile of GlioVac (Figure S6, Supporting Information). Furthermore, we observed a significant activation in DC maturation in the CLNs when compared to GlioVac and control groups (Figure S7, Supporting Information). These results suggest that systemic vaccination of GlioVac

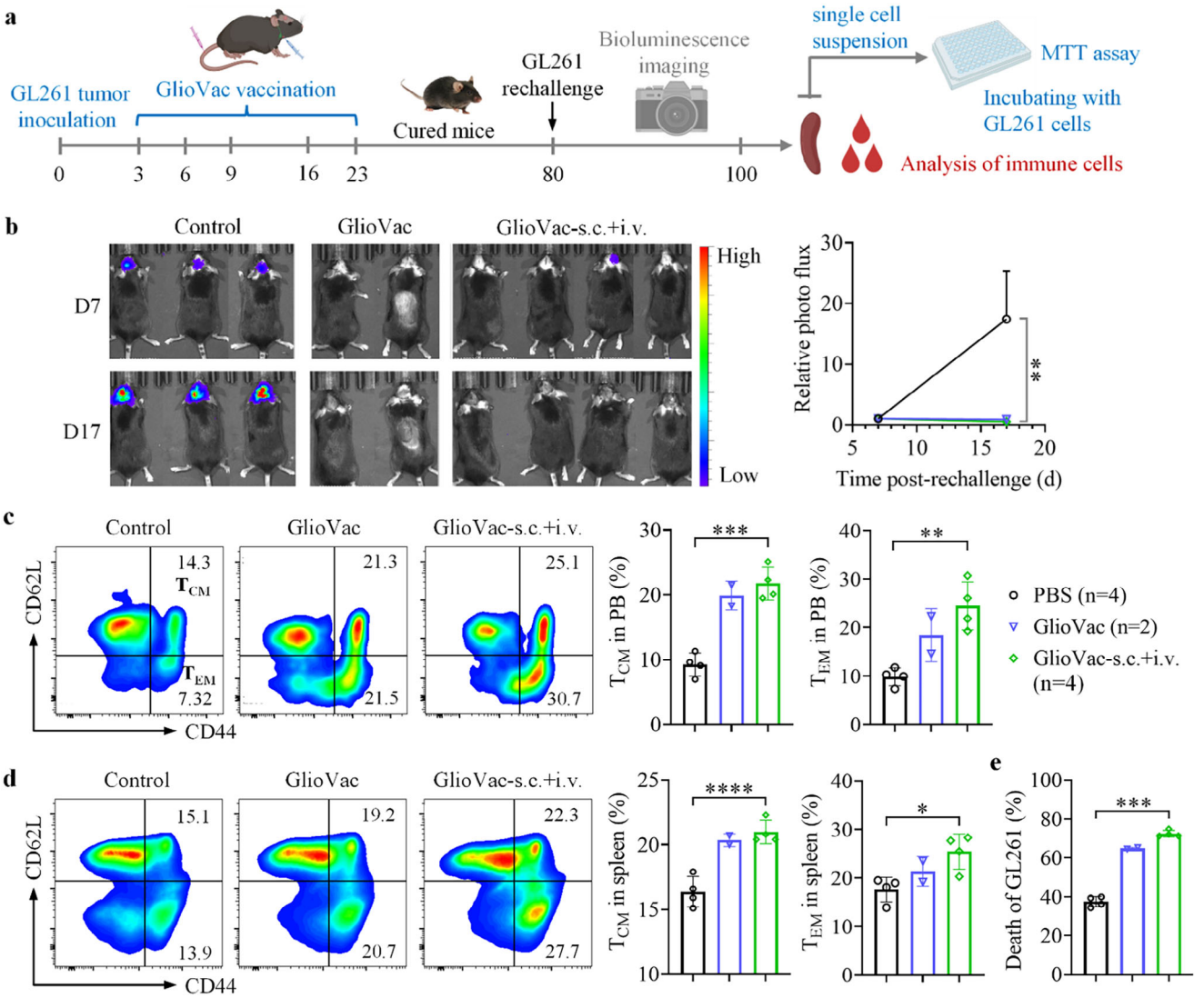

Figure 6. Analyses of immune memory of orthotopic GL261 mice. a) Experimental schedule. Cured mice treated with GlioVac ($n = 2$) and GlioVac-s.c.+i.v. ($n = 4$) were rechallenged on day 80 and analyzed on day 100. Naïve mice intracranially injected with GL261-Luc cells were used as control ($n = 4$). b) Bioluminescence images and relative photo flux of GL261-Luc of mice on days 7 and 17 post-rechallenge. c) Flow charts and percentages of T_{CM} and T_{EM} in PB. d) Flow charts and percentages of $CD44^+CD62L^+T_{CM}$ and $CD44^+CD62L^-T_{EM}$ out of CD3 in the spleen of rechallenged mice. e) Cytotoxicity of splenic cells collected from these mice toward GL261 cells. $^*p < 0.05$, $^{**}p < 0.01$, $^{***}p < 0.001$, $^{****}p < 0.0001$.

is crucial for enerating long-lasting immune memory and enhancing the efficacy of interventions against GBM recurrence. The sequential vaccination of s.c. followed by i.v. not only capitalizes on the strengths of both delivery methods but also promotes synergistic immune activation, thereby fortifying the long-term anti-tumor immunity capable of mounting effective responses to future tumor challenges.

2.7. Immunotherapeutic Efficacy of GlioVac in Viral Plasmid-Induced GBM

We further investigated the therapeutic efficacy of GlioVac using a virus-induced primary GBM model, denoted as hRas-GBM, which was established by injecting virus plasmid encoding tumorigenic gene into the lateral ventricle of C57BL/6J mice, resulting in over-expression of hRas protein and down-expression of p53 in brain cells. Similar to our previous observations, GlioVac that co-delivers CpG and antigens derived from hRas-GBM cell lysates effectively stimulated the maturation of BMDCs (Figure S8a,b, Supporting Information) and promoted their antigen presentation capacity (Figure S8c,d, Supporting Information), demonstrating superior efficacy compared to monotherapies and non-codelivery vaccines. Orthotopic hRas-GBM mice were treated with five s.c. injections of GlioVac (Ag and CpG doses of 0.5 and 1.0 mg kg^{-1}, respectively) to study the anti-GBM efficacy (**Figure 7a**). Survival results showed that GlioVac-s.c. achieved excellent antitumor efficacy with a remarkable 100% GBM elimination without body weight loss during treatment (Figure 7b). In contrast, NanoCpG, NanoAg, and Nano/Ag&CpG

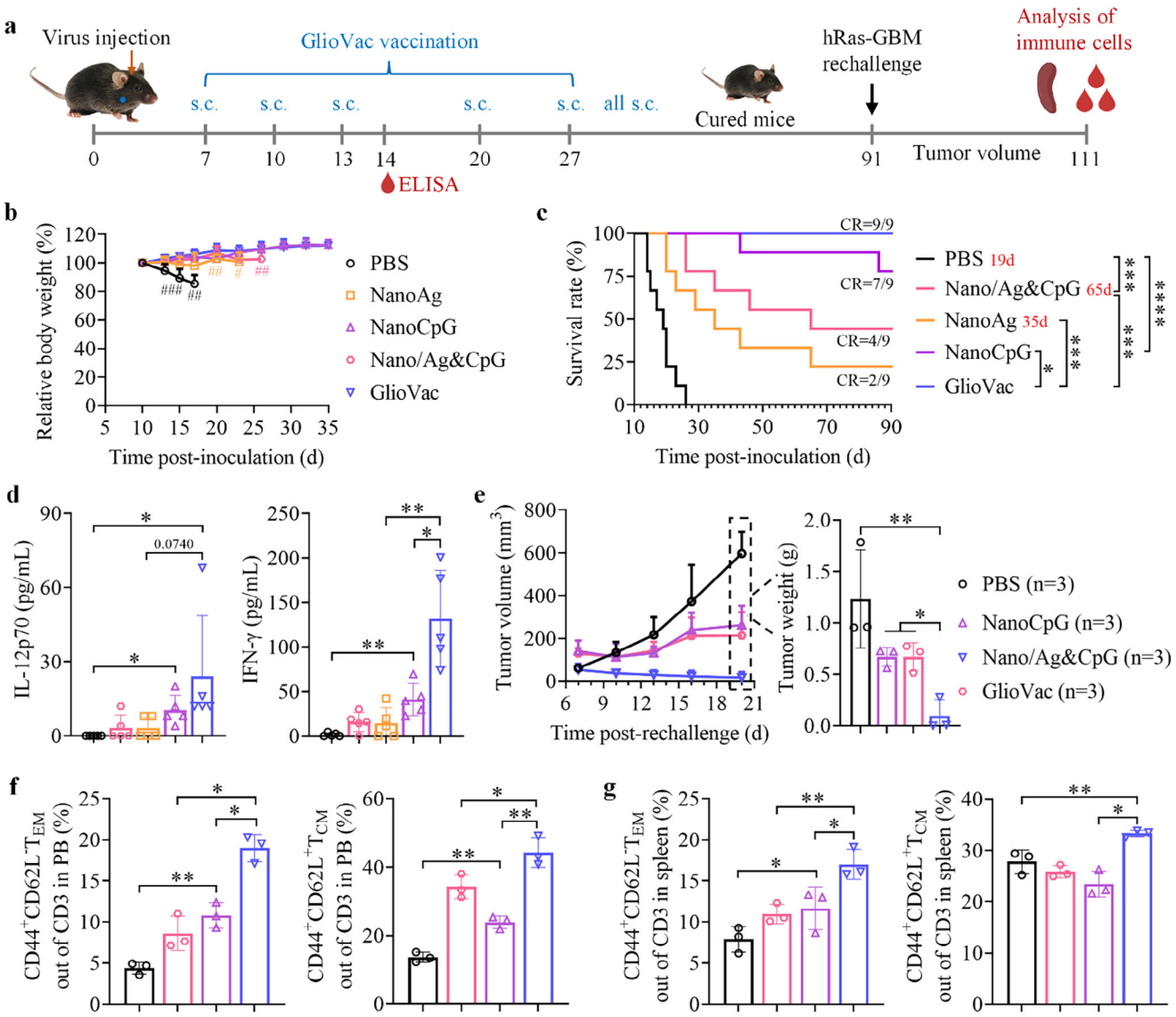

Figure 7. Immunotherapeutic efficacy of GlioVac-s.c. in orthotopic hRas-GBM mice induced by lentiviral plasmid. a) Experimental schedule. On days 7, 10, 13, 20, and 27, mice were s.c. injected with GlioVac, NanoAg, NanoCpG, Nano/Ag&CpG (Ag: 0.5 mg kg^{-1} and CpG: 1 mg kg^{-1}) or PBS. b) Relative body weight and c) survival curves of the mice ($n = 9$). d) Serum concentrations of IL-12p70 and IFN-γ on day 14 ($n = 5$). After hRas-GBM tumor rechallenge on day 91, e) tumor growth curve and tumor weight of rechallenged mice, and percentages of T_{EM} and T_{CM} in the f) PB and g) spleen on day 20 post-rechallenge ($n = 3$). $^{*}p < 0.05$ and $^{**}p < 0.01$.

resulted in tumor-free rates of 44.4%, 77.8%, and 22.2%, respectively (Figure 7c). Moreover, GlioVac led to significantly increased serum levels of IL-12p70 and IFN-γ, verifying systemic immunity activation (Figure 7d). It is observed that NanoCpG and GlioVac demonstrated clearly enhanced therapeutic efficacy in hRas-GBM mice compared to GL261 mice. This improvement is attributed to the "hotter" immune microenvironment in virus-induced models.[23] This was evidenced by the 1.9 and 4.9 fold increase in the expressions of TLR9 and MHC I on hRas-GBM cells, respectively, compared to GL261 cells (Figure S9, Supporting Information).

To assess GlioVac's efficacy against GBM recurrence, three cured hRas-GBM mice were rechallenged with hRas-GBM cells 91 days following the virus injection. Mice that have been cured by NanoCpG and Nano/Ag&CpG treatments showed inhibited tumor progression, although they failed to halt GBM recurrence. Remarkably, GlioVac-cured mice demonstrated maximal suppression of GBM progression, with no recurrence in 2 out of 3 mice within 20 days post-rechallenge (Figure 7e). Moreover, T_{CM} and T_{EM} in the PB and spleen of the GlioVac group were significantly upregulated compared to control groups, with increases ranging from 1.4 to 2.5 fold and 1.1 to 1.9 fold, respectively (Figure 7f,g), demonstrating the generation of long-term immune memory against hRas-GBM recurrence.

To investigate whether GlioVac vaccination could elicit GBM-specific T-cell memory, we rechallenged three cured hRas-GBM

mice that previously received treatment of GlioVac or NanoCpG with GL261 cells (1×10^6) via s.c. injection (Figure S10a, Supporting Information). Notably, all GL261 rechallenged mice in the GlioVac group remained tumor-free, while control mice and 2 out of 3 mice in the NanoCpG group exhibited rapid tumor growth (Figure S10b, Supporting Information), suggesting the importance of tumor-specific antigens in eliciting effective immune responses. GlioVac strengthened T-cell immune memory with upregulation of T_{CM} and T_{EM} in both PB and spleen (Figure S10c,d, Supporting Information), efficiently inhibiting GBM recurrence. However, all mice rechallenged with lung cancer LLC cells showed rapid tumor growth (Figure S10e, Supporting Information), indicating that the immune memory activated by GlioVac based on hRas-GBM antigens could not recognize and respond to LLC cells. This discrepancy may be attributed to differences in surface antigens among various cancers. Although GlioVac may not spread antigen coverage to other types of tumors, it effectively activates GBM-specific immune responses and amplifies the targeting of GBM antigens.

We further investigated the efficacy of GlioVac in advanced orthotopic hRas-GBM mice established with doubled virus titers (Figure S11a, Supporting Information). GlioVac exhibited excellent survival benefits with an 83% tumor-free rate (Figure S11b,c, Supporting Information) and effectively mitigated tumor recurrence (Figure S11d, Supporting Information). These results confirm that GlioVac induces significant regression in various GBM models, demonstrating its potential as a personalized nanovaccine for clinical therapy against GBM.

3. Conclusion

We have demonstrated that a GBM cell lysate nanovaccine boosted with TLR9 agonist CpG ODN (GlioVac) via a strategic vaccination regimen regresses malignant murine GBM tumors. GlioVac demonstrates superior accumulation in the CLNs and enhanced uptake in APCs following s.c. injection near CLNs, which results in significant DC maturation and antigen presentation capacity, as well as a robust local immune activation with enhanced tumor infiltration of GBM-specific CTLs. The i.v. administration of GlioVac reinforces their accumulation in the spleen and lymph nodes. Notably, the sequential s.c. and i.v. vaccination regimen of GlioVac (GlioVac-s.c.+i.v.) further strengthens therapeutic outcomes and successfully activates systemic innate and adaptive immune responses in orthotopic GL261 models, leading to a noteworthy 71% tumor-free survival and 100% long-term protection. Current nanovaccines do carry the risk of immune side effects due to the presence of unknown antigen components and proteins/nucleic acids found in normal cells. However, the unique antigens characteristic of GBM, coupled with the adeptness of DCs in selective presention of these immunogenic tumor antigens, significantly reduce the likelihood of unintended targeting of normal glial cells. GlioVac showcases a straightforward and controllable preparation, demonstrating significant potential in personalized immunotherapy tailored to the unique characteristics of GBM via rational vaccination, thus holding promise for clinical GBM treatment.

4. Experimental Section

Preparation of GlioVac: GlioVac was fabricated facilely through the self-assembly of PEG-P(TMC-DTC)-Spe (40 mg mL^{-1} in 100 µL DMF) in GBM tumor cell lysate (TCL) and/or CpG ODN solution (200 µg each) in phosphate buffer (PB, 2 mM, pH 6.0, 900 µL) following with dialysis (MWCO 1000 kDa). Empty polymersomes (vehicle), and nanopolymersomes loaded with TCL-based antigen (NanoAg) or with CpG (NanoCpG) were prepared by the same method and applied as controls. Size distribution, zeta potential, drug loading content, and stability of GlioVac were determined using Zetasizer Nano-ZS, transmission electron microscopy, Nanodrop, microBCA assays, and agarose gel electrophoresis.

In Vitro Activation of Immune Cells Induced by GlioVac: BMDCs were cultured in 24-well plate (1×10^6/well) and treated with GlioVac, NanoAg, NanoCpG, free Ag&CpG, or Nano/Ag&CpG (a mixture of vehicle and free Ag&CpG) (Ag and CpG conc.: 1 µg mL^{-1}, PBS as control, $n = 3$). After 24 h incubation, TNF-α and IL-12p70 in culture medium were quantified using ELISA, and BMDCs were blocked with murine CD16/32 antibody for 20 min, and stained with FITC-anti-CD11c, PE-anti-CD86, APC-anti-CD80, PE/Cy7-anti-MHC I, and Percp/Cy5.5-anti-MHC II for 30 min at 4 °C. Cells were measured using flow cytometry (FC) and analyzed using FlowJo software.

Splenic single cells were collected from healthy female C57BL/6J mice using standard procedure and implanted in a 12-well plate containing RPMI-1640 medium (5×10^6/well). GlioVac, NanoAg, NanoCpG, free Ag&CpG, or Nano/Ag&CpG (Ag and CpG conc.: 1 µg mL^{-1}) were added to culture for 48 h ($n = 3$, PBS as control). Cells were stained with Zombie NIR Fixable Viability Kit and blocked with anti-CD16/32. Cells were then stained with Percp/Cy5.5-anti-CD45, FITC-anti-CD3, and PE/Cy7-anti-CD8a at 4 °C for 30 min, permeabilized with foxp3/transcription factor staining buffer kit for 60 min, and stained with APC-anti-IFN-γ at room temperature for 30 min followed by FC measurements.

Biodistribution of GlioVac in Orthotopic GL261 Mice: All animal experiments were approved by the Animal Care and Use Committee of Soochow University (P. R. China) and all protocols for the animal studies conformed to the Guide for the Care and Use of Laboratory Animals (approval numbers: 202208A0588, 202212A0269, 202302A0432, 202305A1009, 202308A0567).

Orthotopic GL261-tumor bearing mouse model (GL261 mice) was established by intracranially injecting 5 µL murine GBM GL261 cells (1×10^5) into the left striatum of 8-week-old female C57BL/6J mice as previously reported.[24] To study biodistribution, five days post-inoculation, Cy5-labeled GlioVac (loading Cy5-labeled CpG, cy5-CpG, as probe) was administrated into GL261 mice via subcutaneous (s.c.) injection near CLNs (s.c.-CLN), s.c. injection near ALNs (s.c.-ALN) or intravenous (i.v.) injection (0.5 µg cy5 per mouse, $n = 3$). At 6 and 12 h post-injection, in vivo fluorescence images of mice were collected, and at 12 h ex vivo fluorescence images of main organs (heart, liver, spleen, lung, and kidney) and lymph nodes (CLNs, ALNs, and ILNs) were acquired using In Vivo Imaging System and semi-quantified using Living Image software.

To investigate the CLN-homing effect and cellular uptake of GlioVac, GL261 mice were treated with 100 µL cy5-labeled GlioVac or free Ag&CpG (0.5 µg cy5 per mouse, $n = 3$) via s.c.-CLN administration. At 4 h post-injection, mice were sacrificed and ex-vivo fluorescence images of CLNs were scanned using IVIS. CLNs, tumor tissue, and the spleen were collected and treated to obtain single cell suspensions, which were treated with Zombie NIR Fixable Viability Kit and anti-CD16/32. Cells were stained with flow antibodies for FC measurements: DCs ($CD45^+CD11c^+$), cDC1 ($CD45^+CD11c^+MHC\text{-}II^+CD103^+$), B cells ($CD45^+B220^+$), and macrophages ($CD45^+CD11b^+F4/80^+$). The mean fluorescence intensity (MFI) of cy5-CpG in various organs and APCs was detected using FC.

Anti-Tumor Efficacy of GlioVac in Orthotopic GL261 Mice: GL261 mice were administered with 100 µL GlioVac, NanoAg, NanoCpG, Nano/Ag&CpG (Ag: 1 mg kg^{-1}, CpG: 1 mg kg^{-1}) or PBS on days 3, 6, 9, 16, 23 post-inoculation ($n = 8$) via s.c. injection near CLNs. GlioVac had also administrated another regimen with the first two s.c.-CLN injections followed by three i.v. injections (denoted as GlioVac-s.c.+i.v.). Body

weight of mice was monitored every 2 days ($n = 7$). On day 10, blood samples were collected to determine serum levels of IFN-γ, IL-12p70, and IL-10 using ELISA kits ($n = 7$). On day 18, one mouse from PBS, GlioVac, and GlioVac-s.c.+i.v. groups were randomly selected to collect the brain and major organs for hematoxylin and eosin (H&E) analysis. The remaining mice were used for survival curves and mouse death or body weight loss over 15% was considered death ($n = 7$).

To study the immune memory generated by GlioVac ($n = 2$) and GlioVac-s.c.+i.v. ($n = 4$), cured mice were intracranially rechallenged with GL261-Luc cells (1×10^5) on day 80 after initial inoculation. Naïve mice intracranially injected with GL261-Luc cells were used as control ($n = 4$). Bioluminescence images and relative photo flux were monitored by IVIS on days 7 and 17 post-rechallenge. On day 20, rechallenged GL261 mice were sacrificed to extract peripheral blood (PB) and spleen for memory immune cell analysis. The prepared single-cell suspensions were labeled with Zombie NIR and blocked with anti-CD16/32. Cells were then labeled with percp/cy5.5-anti-CD45, APC-anti-CD3, PE/Cy7-anti-CD4, PE/Cy7-anti-CD8, FITC-anti-CD44 and PE-anti-CD62L before FC measurements.

To detect the cytotoxicity of splenic cells against GL261 cells, splenic cells (5×10^4) were extracted from surviving mice previously treated with GlioVac or GlioVac-s.c.+i.v. as above, and co-cultured with GL261 cells (5×10^3) in 96-well plates for 48 h. After removing the medium containing splenic cells, GL261 cells were washed and replenished with RPMI-1640 medium. 10 µL MTT (5 mg mL^{-1}) was added to incubate for 4 h at 37 °C. The purple crystals were dissolved with 150 µL DMSO, and the absorbance at 570 nm was measured using a microplate reader. Cell viability (%) was determined by comparing the absorbance at 570 nm with control wells of GL261 cells added with PBS but without splenic cells (100% viability).

Immunological Analysis of Orthotopic GL261 Mice Treated by GlioVac: GL261 mice were administered with GlioVac, NanoAg, NanoCpG, Nano/Ag&CpG, or PBS via s.c. injection near CLNs on days 3, 6, 9, and 16 post-inoculation ($n = 7$). GlioVac-s.c.+i.v. regimen was also conducted with the first two s.c.-CLN injects followed by two i.v. injections. On day 18, one mouse from each group was randomly selected to prepare brain slices for immunohistochemistry (IHC) assay. The slices were dewaxed, rehydrated, treated with an antigenic repair agent, and blocked with goat serum (room temperature, 1 h). The slices were then stained overnight with CD80 antibody (DCs), CD3 and CD8 antibodies (CD8$^+$T cells), NKR-P1C antibody (NK cells), Iba1 antibody (Mϕ, macrophage), and iNOS antibody (M1M), followed by treating with Alexa Fluor 647 goat anti-rabbit IgG H&L secondary antibody (Alexa Fluor 488 labeling for CD3 and Iba1) for 2 h and imaging with CLSM. The remaining six mice of each group were sacrificed to collect peripheral blood, tumor, CLNs, and spleen to make single-cell suspensions for determining DCs, macrophages, T cells, B cells, NK cells, and NKT cells using FC (detailed treatment in SI).

Statistical Analysis: All data were represented as mean ± standard deviation. Significant differences among groups were calculated using one-way ANOVA followed by Tukey's multiple comparison tests using GraphPad Prism 8.0. One-way ANOVA using a log-rank test was applied for the Kaplan–Meier survival rates analysis. Statistical significance was defined as follows: $^*p < 0.05$, $^{**}p < 0.01$, $^{***}p < 0.001$ and $^{****}p < 0.0001$.

Supporting Information

Supporting Information is available from the Wiley Online Library or from the author.

Acknowledgements

This work is supported by research grants from the National Natural Science Foundation of China (NSFC 52473142, 52233007, 52033006) and the National Key R&D Program of China (2022YFA1206000). The authors thank Biorender.com for the assistance in illustrations.

Conflict of Interest

The authors declare no conflict of interest.

Data Availability Statement

The data that support the findings of this study are available from the corresponding author upon reasonable request.

Keywords

brain tumor, immunoadjuvant, lymph node-targeting, nanovaccines, personalized vaccines

Received: February 19, 2025
Revised: April 2, 2025
Published online: April 24, 2025

[1] a) D. N. Louis, A. Perry, P. Wesseling, D. J. Brat, I. A. Cree, D. Figarella-Branger, C. Hawkins, H. K. Ng, S. M. Pfister, G. Reifenberger, R. Soffietti, A. von Deimling, D. W. Ellison, *Neuro-Oncology* **2021**, *23*, 1231; b) R. McLendon, *Nature* **2008**, *455*, 1061.

[2] a) T. I. Janjua, P. Rewatkar, A. Ahmed-Cox, I. Saeed, F. M. Mansfeld, R. Kulshreshtha, T. Kumeria, D. S. Ziegler, M. Kavallaris, R. Mazzieri, A. Popat, *Adv. Drug Delivery Rev.* **2021**, *171*, 108; b) J. Xue, Z. Zhao, L. Zhang, L. Xue, S. Shen, Y. Wen, Z. Wei, L. Wang, L. Kong, H. Sun, Q. Ping, R. Mo, C. Zhang, *Nat. Nanotechnol.* **2017**, *12*, 692.

[3] a) M. Weller, P. Roth, M. Preusser, W. Wick, D. A. Reardon, M. Platten, J. H. Sampson, *Nat. Rev. Neurol.* **2017**, *13*, 363; b) D. B. Keskin, A. J. Anandappa, J. Sun, I. Tirosh, N. D. Mathewson, S. Li, G. Oliveira, A. Giobbie-Hurder, K. Felt, E. Gjini, S. A. Shukla, Z. Hu, L. Li, P. M. Le, R. L. Allesøe, A. R. Richman, M. S. Kowalczyk, S. Abdelrahman, J. E. Geduldig, S. Charbonneau, K. Pelton, J. B. Iorgulescu, L. Elagina, W. Zhang, O. Olive, C. McCluskey, L. R. Olsen, J. Stevens, W. J. Lane, A. M. Salazar, et al., *Nature* **2018**, *565*, 234.

[4] F. Hameedat, B. B. Mendes, J. Conniot, L. D. Di Filippo, M. Chorilli, A. Schroeder, J. Conde, F. Sousa, *Nat. Rev. Mater.* **2024**, *9*, 628.

[5] L. M. Liau, K. Ashkan, S. Brem, J. L. Campian, J. E. Trusheim, F. M. Iwamoto, D. D. Tran, G. Ansstas, C. S. Cobbs, J. A. Heth, M. E. Salacz, S. D'Andre, R. D. Aiken, Y. A. Moshel, J. Y. Nam, C. P. Pillainayagam, S. A. Wagner, K. A. Walter, R. Chaudhary, S. A. Goldlust, I. Y. Lee, D. A. Bota, H. Elinzano, J. Grewal, K. Lillehei, T. Mikkelsen, T. Walbert, S. Abram, A. J. Brenner, M. G. Ewend, et al., *JAMA Oncol.* **2023**, *9*, 112.

[6] M. S. Ahluwalia, D. A. Reardon, A. P. Abad, W. T. Curry, E. T. Wong, S. A. Figel, L. L. Mechtler, D. M. Peereboom, A. D. Hutson, H. G. Withers, S. Liu, A. N. Belal, J. X. Qiu, K. M. Mogensen, S. S. Dharma, A. Dhawan, M. T. Birkemeier, D. M. Casucci, M. J. Ciesielski, R. A. Fenstermaker, *J. Clin. Oncol.* **2023**, *41*, 1453.

[7] a) T. Fan, M. Zhang, J. Yang, Z. Zhu, W. Cao, C. Dong, *Signal Transduct. Target. Ther.* **2023**, *8*, 450; b) S. Zhou, Y. Huang, Y. Chen, Y. Liu, L. Xie, Y. You, S. Tong, J. Xu, G. Jiang, Q. Song, N. Mei, F. Ma, X. Gao, H. Chen, J. Chen, *Nat. Commun.* **2023**, *14*, 435; c) M. Gromeier, M. C. Brown, G. Zhang, X. Lin, Y. Q. Chen, Z. Wei, N. Beaubier, H. Yan, Y. P. He, A. Desjardins, J. E. Herndon, F. S. Varn, R. G. Verhaak, J. F. Zhao, D. P. Bolognesi, A. H. Friedman, H. S. Friedman, F. McSherry, A. M. Muscat, E. S. Lipp, S. K. Nair, M. Khasraw, K. B. Peters, D. Randazzo, J. H. Sampson, R. E. McLendon, D. D. Bigner, D. M. Ashley, *Nat. Commun.* **2021**, *12*, 352.

[8] a) F. Cheng, T. Su, S. Zhou, X. Liu, S. Yang, S. Lin, W. Guo, G. Zhu, *Sci. Adv.* **2023**, *9*, ade6257; b) F. Chen, T. Li, H. Zhang, M. Saeed, X. Liu, L. Huang, X. Wang, J. Gao, B. Hou, Y. Lai, C. Ding, Z. Xu, Z. Xie, M. Luo, H. Yu, *Adv. Mater.* **2023**, *35*, 2209910; c) S. Zhang,

F. Raza, L. Jiang, J. Su, W.-E. Yuan, M. Qiu, *Nano Today* **2024**, *57*, 102321.

[9] a) Y. K. Li, H. Q. Zhang, R. K. Wang, Y. Wang, R. A. Li, M. S. Zhu, X. Y. Zhang, Z. Zhao, Y. J. Wan, J. Zhuang, H. K. Zhang, X. L. Huang, *Adv. Mater.* **2023**, *35*, 2208923; b) Z. Meng, Y. Zhang, X. Zhou, J. Ji, Z. Liu, *Adv. Drug Delivery Rev.* **2022**, *182*, 114107.

[10] T. Wang, M. Han, Y. Han, Z. Jiang, Q. Zheng, H. Zhang, Z. Li, *ACS Nano* **2024**, *18*, 6333.

[11] a) F. Baharom, R. A. Ramirez-Valdez, A. Khalilnezhad, S. Khalilnezhad, M. Dillon, D. Hermans, S. Fussell, K. K. S. Tobin, C.-A. Dutertre, G. M. Lynn, S. Müller, F. Ginhoux, A. S. Ishizuka, R. A. Seder, *Cell* **2022**, *185*, 4317; b) F. Baharom, R. A. Ramirez-Valdez, K. K. S. Tobin, H. Yamane, C.-A. Dutertre, A. Khalilnezhad, G. V. Reynoso, V. L. Coble, G. M. Lynn, M. P. Mulè, A. J. Martins, J. P. Finnigan, X. M. Zhang, J. A. Hamerman, N. Bhardwaj, J. S. Tsang, H. D. Hickman, F. Ginhoux, A. S. Ishizuka, R. A. Seder, *Nat. Immunol.* **2020**, *22*, 41.

[12] a) G. Cui, Y. Sun, L. Qu, C. Shen, Y. Sun, F. Meng, Y. Zheng, Z. Zhong, *Adv. Healthcare Mater.* **2024**, *13*, 2303690; b) P. Zhang, T. Wang, G. Cui, R. Ye, W. Wan, T. Liu, Y. Zheng, Z. Zhong, *Adv. Mater.* **2024**, *36*, 2407189.

[13] a) L. Wang, C. Zhang, J. Zhao, Z. Zhu, J. Wang, W. Fan, W. Jia, *Adv. Mater.* **2024**, *36*, 2308110; b) X. Zhao, Y. Dong, J. Zhang, C. Chen, L. Gao, C. Shi, Z. Fu, M. Han, C. Tang, P. Sun, Z. Yang, C. Zhang, K. Zhao, X. Jiang, *Acta Biomater.* **2023**, *166*, 512.

[14] a) O. P. Joffre, E. Segura, A. Savina, S. Amigorena, *Nat. Rev. Immunol.* **2012**, *12*, 557; b) P. Rodríguez-Silvestre, M. Laub, P. A. Krawczyk, A. K. Davies, J. P. Schessner, R. Parveen, B. J. Tuck, W. A. McEwan, G. H. H. Borner, P. Kozik, *Science* **2023**, *380*, 1258.

[15] Y. Miao, L. Niu, X. Lv, Q. Zhang, Z. Xiao, Z. Ji, L. Chen, Y. Liu, N. Liu, J. Zhu, Y. Yang, Q. Chen, *Adv. Mater.* **2024**, *36*, 2410715.

[16] a) Y. Qi, W. Xiong, Q. Chen, Z. Ye, C. Jiang, Y. He, Q. Ye, *J. Nanobiotechnology* **2023**, *21*, 254; b) E. Song, T. Mao, H. Dong, L. S. B. Boisserand, S. Antila, M. Bosenberg, K. Alitalo, J. L. Thomas, A. Iwasaki, *Nature* **2020**, *577*, 689.

[17] a) G. Zhu, F. Zhang, Q. Ni, G. Niu, X. Chen, *ACS Nano* **2017**, *11*, 2387; b) T. Cai, H. Liu, S. Zhang, J. Hu, L. Zhang, *J. Nanobiotechnology* **2021**, *19*, 389.

[18] J. R. Ohlfest, B. M. Andersen, A. J. Litterman, J. Xia, C. A. Pennell, L. E. Swier, A. M. Salazar, M. R. Olin, *J. Immunol.* **2013**, *190*, 613.

[19] a) S. C. Eisenbarth, *Nat. Rev. Immunol.* **2019**, *19*, 89; b) H. Wang, R. Medina, J. Ye, Y. Zhang, S. Chakraborty, A. Valenzuela, O. Uher, K. Hadrava Vanova, M. Sun, X. Sang, D. M. Park, J. Zenka, M. R. Gilbert, K. Pacak, Z. Zhuang, *Adv. Sci.* **2024**, *11*, 2308280.

[20] T. Wang, H. Zhang, Y. Han, Q. Zheng, H. Liu, M. Han, Z. Li, *Adv. Sci.* **2023**, *10*, 2204961.

[21] a) P. Meiser, M. A. Knolle, A. Hirschberger, G. P. de Almeida, F. Bayerl, S. Lacher, A.-M. Pedde, S. Flommersfeld, J. Hönninger, L. Stark, F. Stögbauer, M. Anton, M. Wirth, D. Wohlleber, K. Steiger, V. R. Buchholz, B. Wollenberg, C. E. Zielinski, R. Braren, D. Rueckert, P. A. Knolle, G. Kaissis, J. P. Böttcher, *Cancer Cell* **2023**, *41*, 1498; b) A. H. Lee, L. Sun, A. Y. Mochizuki, J. G. Reynoso, J. Orpilla, F. Chow, J. C. Kienzler, R. G. Everson, D. A. Nathanson, S. J. Bensinger, L. M. Liau, T. Cloughesy, W. Hugo, R. M. Prins, *Nat. Commun.* **2021**, *12*, 6938.

[22] L. Liu, J. Chen, H. Zhang, J. Ye, C. Moore, C. Lu, Y. Fang, Y.-X. Fu, B. Li, *Nat. Cancer* **2022**, *3*, 437.

[23] a) M. DuPage, A. L. Dooley, T. Jacks, *Nat. Protoc.* **2009**, *4*, 1064; b) A. T. Yeo, S. Rawal, B. Delcuze, A. Christofides, A. Atayde, L. Strauss, L. Balaj, V. A. Rogers, E. J. Uhlmann, H. Varma, B. S. Carter, V. A. Boussiotis, A. Charest, *Nat. Immunol.* **2022**, *23*, 971.

[24] J. Wei, D. Wu, S. Zhao, Y. Shao, Y. Xia, D. Ni, X. Qiu, J. Zhang, J. Chen, F. Meng, Z. Zhong, *Adv. Sci.* **2022**, *9*, 2103689.